JOURNAL OF APPLIED ELECTROCHEMISTRY 21 (1991) 440–445

Electrocatalytic activity of nickel black electrodes for the hydrogen evolution reaction in alkaline solutions

A. C. CHIALVO, M. R. GENNERO DE CHIALVO

Programa de Electroquímica Aplicada e Ingeniería Electroquímica (PRELINE), Facultad de Ingeniería Química (UNL), Santiago del Estero 2829, (3000) Sante Fe, Argentina

Received 31 July 1990; Revised 11 October 1990

The electrocatalytic activity of nickel black electrodes for the hydrogen evolution reaction (HER) in alkaline solutions was studied. Three types of electrode were obtained through electrodeposition from different plating baths and their electrocatalytic properties were evaluated through slow potentiodynamic sweeps. The apparent and real exchange current densities and the Tafel slopes were calculated and compared to those of Raney nickel electrodes. The importance of the superficial topography on the apparent electrocatalytic characteristics was emphasized and some evidence was given to demonstrate that, when the electrode is previously aged in alkaline solution, the HER is produced on a thin nickel hydroxide overlayer.

1. Introduction

It is well known that the materials to be used as cathodes for the hydrogen evolution reaction (HER) in alkaline solutions should have the following characteristics: (i) High apparent exchange current densities (i_0^{ap}) together with low dE/d log i (i.e. Tafel slope, b) values and (ii) high real surface areas [1–3]. Both properties are closely related. Nevertheless, it must be taken into account that both properties are influenced by the topography and the microscopic characteristics of the electrode surface. This fact particularly affects the electrode behaviour in the high overpotential region, where an appropriate surface topography significantly reduces the cathodic overpotential for the HER.

These factors support the idea of using nickel black electrodes as electrocatalysts, because the superficial morphology can be varied by using different electrodeposition media and/or varying the electroplating conditions. The present work studies the electrocatalytic characteristics of nickel electrodeposits obtained from three different deposition baths for the HER in alkaline solutions.

2. Experimental details

Experiments were carried out in a three compartment Pyrex glass cell. The working electrodes consisted of nickel wires (0.4–0.8 cm^2 geometric area), which were previously subjected to an electrodeposition process in order to obtain a nickel black electrodeposit. The counterelectrode was a large area platinum wire. Potentials were measured against the Hg/HgO reference electrode in the same electrolyte solution and are given with respect to the reversible hydrogen electrode (RHE) in the same solution. Special attention was paid to the construction and location of the Luggin–Haber tip, so as to ensure negligible ohmic drops in solution. Experiments were carried out in 2 M NaOH solutions, which were prepared with triply distilled water and purified in the cell by electrolysis with an auxiliary electrode of large surface area. Before each run the solution was saturated with hydrogen. All measurements were made at 30.0 $\pm$ 0.1° C.

Nickel black electrodes were prepared by galvanostatic electroplating of nickel wires in three different baths. The corresponding compositions and electrodeposition conditions are described in Table 1. The nickel substrates were previously etched in a 2 : 1 mixture of acetic and nitric acids. A large area nickel wire spiral concentrically surrounding the working electrode was used as counterelectrode. Bath III was prepared by saturation of a fused 75 wt % NaOH solution with nickel hydroxide at 100° C (at room temperature this mixture is solid). The Teflon cell used for the electroplating process in this bath is shown in Fig. 1.

After the electrodeposition process, the electrodes were rinsed repeatedly with triply distilled water and left for a day in water and another day in 2 M NaOH solution. Before the electrocatalytic evaluation, the electrode was subjected to a triangular potential sweep (t.p.s.) run at 0.1 $V s^{-1}$ between -0.5 V and 0.65 V against Hg/HgO and the corresponding potentiodynamic $i - E$ profile was recorded. From this voltammogram, the electroreduction oxide charge of Ni(III) species was calculated.

The HER study consisted of a slow potentiodynamic sweep (10^{-4} $V s^{-1}$) from -0.05 V to -0.4 V, run after a potentiostatization step at -0.3 V for 1 min. Then, the electrode was subjected to a t.p.s. in the same conditions as described above. The electroreduction oxide charge calculated from the corresponding voltammogram was, for all types of electrode studied, identical to that obtained before the electrocatalytic

0021-891X/91 $03.00 + .12

Table 1. Composition of the plating baths and electrodeposition conditions for the preparation of the different types of nickel black electrodes

Electrode	*Bath composition*	*Plating conditions*
I	Nickel citrate 10 g dm^{-3}	Temperature: 25° C
	Ammonium sulphate 50 g dm^{-3}	Current density: 20 mA cm^{-2}
	Ammonium hydroxide (pH 9.8)	Time: 0.5–3 h
II	Nickel sulphate 35 g dm^{-3}	Temperature: 25° C
	Ammonium sulphate 33 g dm^{-3}	Current density: 40 mA cm^{-2}
	Sulphuric acid (pH 4.4)	Time: 0.2–3 h
III	Sodium hydroxide 75 wt %	Temperature: 100° C
	Water 25 wt %	Current density: 10 mA cm^{-2}
	Nickel hydroxide (saturation)	Time: 0.2–3 h

determination. The values of the current density (i), apparent exchange current density (i_0^{ap}) and the oxide charge (Q) were referred to the geometric electrode area. SEM micrographs of the different types of nickel black electrodes were also obtained using a JEOL JM-35C scanning electron microscope.

3. Results

The dependence of the logarithm of the current density on the overpotential (log i against η) was obtained from the slow potentiodynamic sweep run in the hydrogen evolution potential range. The results obtained for the three types of nickel black electrodes are depicted in Figs 2–4. Each figure shows the response of electrodes prepared at different times of deposition.

The electrodes of type I, which were obtained by

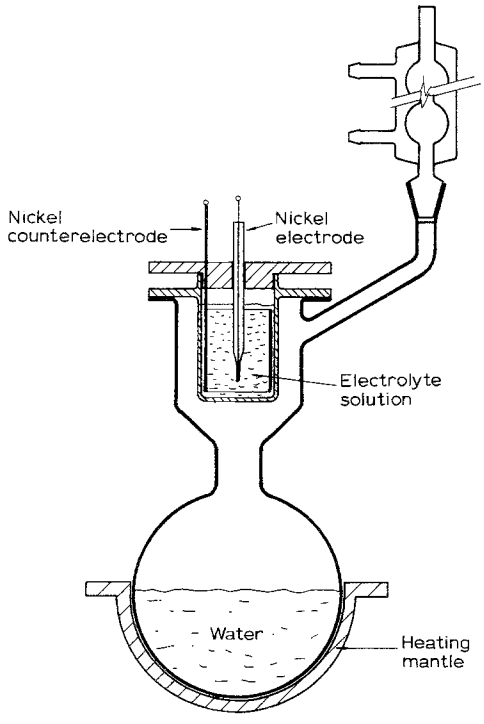

Fig. 1. Schematic representation of the electroplating cell for the preparation of type III electrodes.

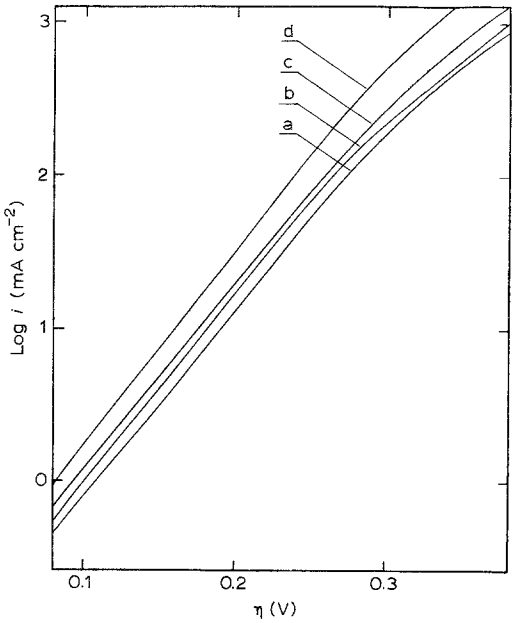

Fig. 2. Tafel plots for HER on type I electrodes with different charges, Q: (a) 32.6, (b) 46.2, (c) 53.5 and (d) 86.5 mC cm^{-2}.

electrodeposition in nickel citrate solutions, show linear log i against η relationships on a wide range of overpotentials (Fig. 2). The corresponding Tafel slope is about 0.080 V dec^{-1} for $\eta > -0.3$ V. On the other hand, the electrodes obtained in the nickel sulphate bath (type II) gave Tafel lines in a potential region narrower than that of the type I electrodes (Fig. 3). For $\eta > -0.25$ V, the Tafel slope is about 0.105 V dec^{-1}. Finally, the electrodes prepared in the fused mixture of sodium and nickel hydroxides (type III) give log i against η relationships which are approximately linear in the region $-0.25\text{ V} < \eta < -0.15$ V and the corresponding b value is about 0.090 V dec^{-1} (Fig. 4).

A direct relation between the current density at a given overpotential and the oxide electroreduction charge for each type of electrode was observed. The latter, which can be considered proportional to the

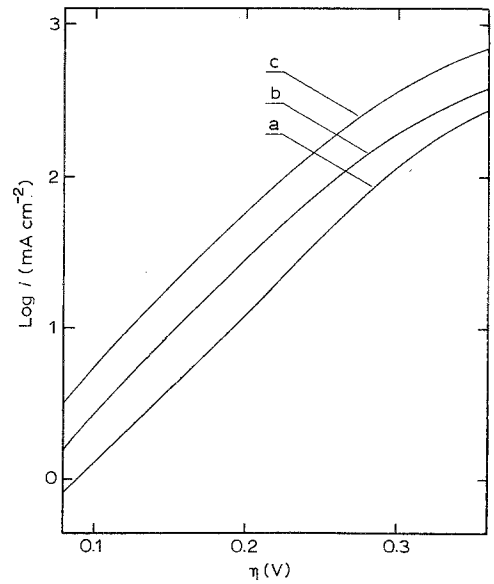

Fig. 3. Tafel plots for HER on type II electrodes with different charges, Q: (a) 37, (b) 119 and (c) 268 mC cm^{-2}.

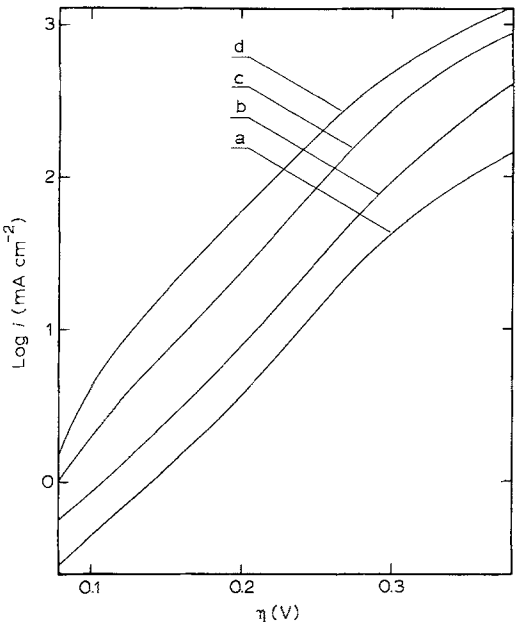

Fig. 4. Tafel plots for HER on type III electrodes with different charges, Q: (a) 16, (b) 47, (c) 175 and (d) 480 mC cm^{-2}.

surface area, is varied by changing the time of the electrodeposition process.

Figs 5–7 show SEM micrographs of the three types of nickel black electrode. Secondary and tertiary nodular growth can be distinguished for type I, producing a typical "cauliflower" structure [4], which is characterized by the development of high surface area (Fig. 5). The type II electrode shows a surface structure similar to that of type I, but in this case the number of nucleation sites is less with a greater growth of individual nodules. Consequently, the real surface area is less (Fig. 6). Finally, the electrodes prepared in the fused NaOH–Ni(OH)$_2$ mixture (type III) show a dendritic "fern-like" structure, with some secondary nodular growth (Fig. 7).

3. Discussion

The present results show that the three types of nickel black electrode have different electrocatalytic activity, evaluated through the Tafel slope, b, for the hydrogen evolution reaction in alkaline solutions. In principle, these differences may be attributed to mass transport

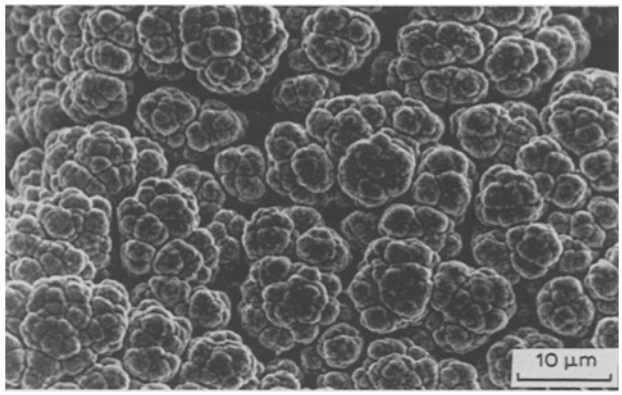

Fig. 6. SEM micrograph of a type II electrode. Deposition time: 30 min. Magnification: 1500×.

processes that take place inside the intersticies of the electrodeposits (Figs 5–7). Nevertheless, the Tafel slope of a smooth nickel electrode for HER [5, 6] in the conditions of the present work is about 0.110 V dec^{-1}, a value which is greater than those obtained here (Table 2). Therefore, the variation is produced in the opposite direction to the expected behaviour [7, 8]. Besides, for a given type of electrode, the migrational and diffusional phenomena should produce an increase in the Tafel slope as the porosity increases. This fact was again not experimentally observed, as can be seen in Figs 2–4. Consequently, it may be concluded that the whole electrode surface is equally attainable for the reactants and that the different behaviour observed must be attributed to the different amount and distribution of active sites on the electrode surface.

In order to calculate the kinetic parameters for each type of nickel black electrode, the existence of a linear dependence between the real surface area and the oxide charge is considered. On this basis, the following expression was used [9] to evaluate the Tafel slope:

$$\log (i/Q) = |\eta|/b + \log i_0 k \qquad (1)$$

and the exchange current density (i_0):

$$i_0^{ap} = i_0(1 + kQ) \qquad (2)$$

The apparent exchange current density (i_0^{ap}) contains the contribution of the roughness factor, while i_0 corresponds specifically to the substrate.

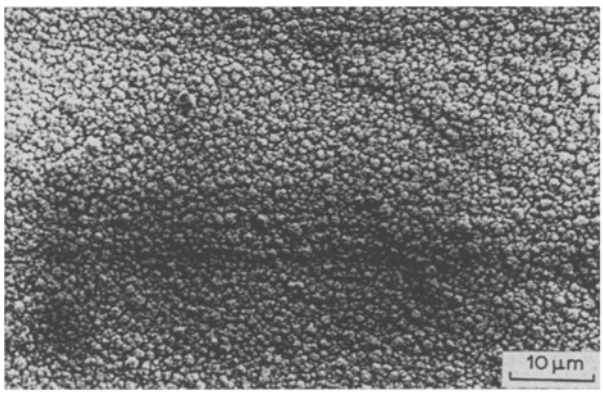

Fig. 5. SEM micrograph of a type I electrode. Deposition time: 30 min. Magnification: 1500×.

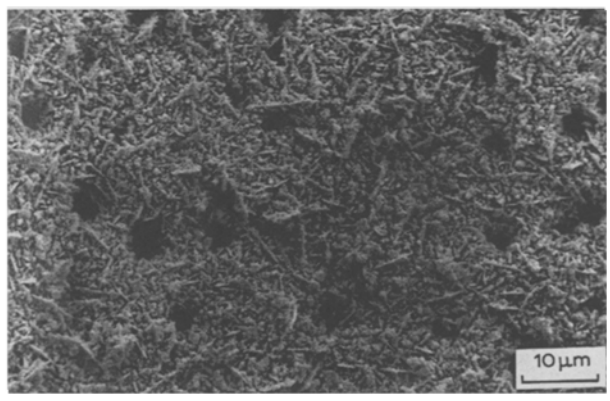

Fig. 7. SEM micrograph of a type III electrode. Deposition time: 30 min. Magnification: 1500×.

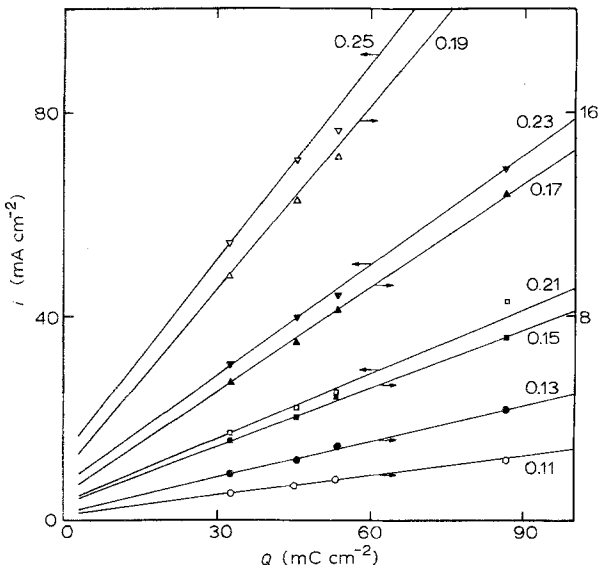

Fig. 8. Dependence of the current density upon the oxide charge at different overpotential values for type I electrodes.

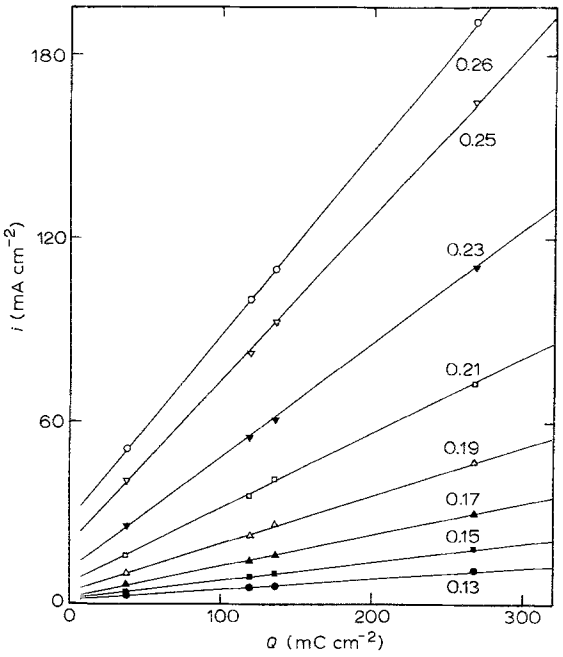

Fig. 9. Dependence of the current density upon the oxide charge at different overpotential values for type II electrodes.

The applicability of Equations 1 and 2 is verified in Figs 8–13. A linear dependence between the current density and the oxide charge for different overpotential values is observed for each type of nickel black electrode (Figs 8–10). With data obtained from these figures, the log (i/Q) against η and i_0^{ap} against Q relationships (Figs 11–13) were plotted and, consequently, the kinetic parameters of each type of electrode were calculated (Table 2). From the results given in this table, the following considerations can be made:

(i) The exchange current densities obtained in this work are similar to those given in the literature [10, 11] for bright nickel electrodes in the same conditions. Nevertheless, as the coverage of the adsorbed hydrogen should be considered approximately constant in the overpotential range analysed but different for each type of electrode, the i_0 values for the three types of nickel black electrodes should not be directly compared.

(ii) The electrodes are covered by a superficial film of $\beta Ni(OH)_2$ developed spontaneously [12, 13] during the immersion in the 2 M NaOH solution previous to the electrocatalytic study. The comparison of the electroreduction oxide charges voltammetrically determined before and after the electrocatalytic evaluation results in identical values. On the other hand, several monolayers of hydrated oxide cannot be regenerated on one potentiodynamic sweep [14]. On this basis, it should be concluded that the superficial layer cannot be electrochemically reduced, which is in agreement with the results obtained by other authors [15]. Therefore, it should be inferred, at least in the present conditions, that the HER takes place on a hydrated oxide overlayer. This assumption, suggested previously by other authors [16, 17], agrees with the values of the constant k experimentally evaluated through Equations 1 and 2. The inverse of this constant represents the oxide charge per unit of the real area $[k^{-1} = \Delta Q/\Delta A(\text{real})]$. Comparing this value with that corresponding to one monolayer $[\Delta Q/\Delta A = 0.5\,\text{mC cm}^{-2}]$ [15], it can be seen that the thickness of the oxide layer of electrodes of types I and III is in the order of 30 monolayers and twice this value for type II. Furthermore, these quantities are consistent with the thickness of oxide layers naturally produced when a polished nickel surface is immersed in an alkaline solution for a long period of time [12, 13].

Table 2. Kinetic parameters for the HER of the different types of nickel black electrodes

Electrode	$i_0 \times 10^5$ $(A\,cm^{-2})$	b $(V\,dec^{-1})$	k^{-1} $(mC\,cm^{-2})$
I	1.45	0.082	13.6
II	8.00	0.105	31.4
III	1.10	0.0908	15.4

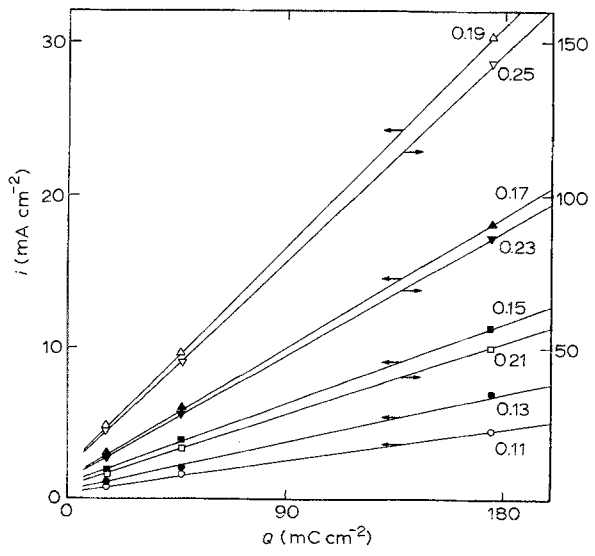

Fig. 10. Dependence of the current density upon the oxide charge at different overpotential values for type III electrodes.

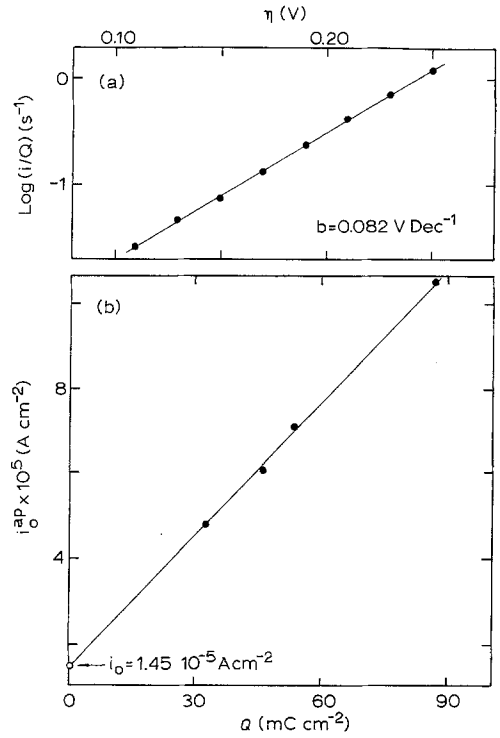

Fig. 11. Dependence of: (a) log (i/Q) against η (values obtained from Fig. 8) and (b) i_0^{ap} against Q for type I electrodes.

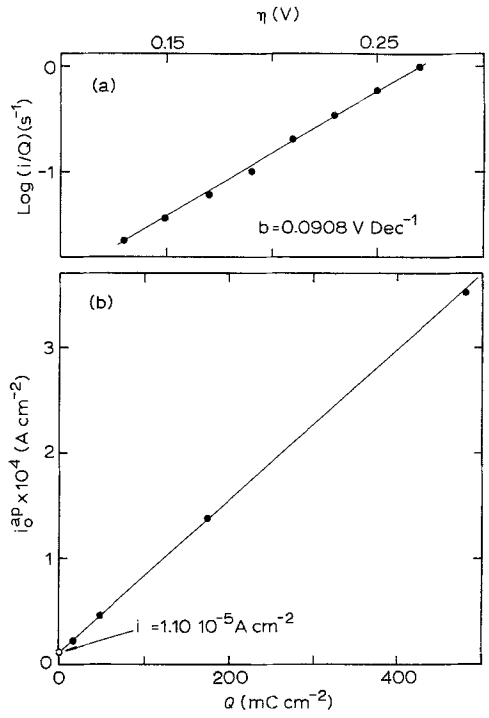

Fig. 13. Dependence of (a) log (i/Q) against η (values obtained from Fig. 10) and (b) i_0^{ap} against Q for type III electrodes.

(iii) Electrodes of type I show excellent electrocatalytic activity, exhibiting a wide range of linearity in the log i against η relationships. A current density of about 0.5 mA cm^{-2} for $\eta = -0.30$ V was obtained for this electrode. This value is similar to that obtained for a certain type of Raney nickel electrode, treated in NaOH or HF solutions, where the roughness factor is in the order of 3000 [18]. It should be interesting to compare the behaviour of these two types of electrode,

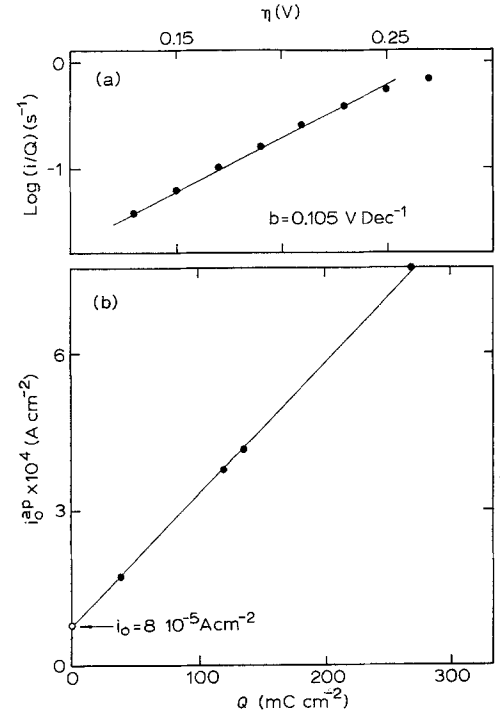

Fig. 12. Dependence of (a) log (i/Q) against η (values obtained from Fig. 9) and (b) i_0^{ap} against Q for type II electrodes.

black and Raney, respectively. Both show a high apparent electrocatalytic activity, originating mainly from the high real area. Nevertheless, the roughness factor of the Raney nickel electrode is substantially greater than that of the nickel black electrodeposit because the high surface area of the former arises from its porous structure, which results in a less efficient use of the whole electrode surface [3, 19]. On the other hand, the superficial morphology of nickel black electrodeposits leads to a more efficient utilization of the available active sites [20].

It may be concluded that, in order to obtain high apparent exchange current densities and low Tafel slope values, it is necessary to develop high real electrode surface areas along with suitable superficial topographies that make all the electroactive sites equally accessible to the reactant. The results described in the present work suggest that these two characteristics are found in the nickel black electrodeposits obtained from the citrate bath. Consequently, further studies must be carried out in order to optimize the morphology of this type of electrode.

Acknowledgements

This work was supported by the Consejo Nacional de Investigaciones Cientificas y Técnicas (CONICET, Argentina) and the Stiftung Volkswagenwerk, Federal Republic of Germany.

References

[1] B. E. Conway and L. Bai, *Int. J. Hydrogen Energy* **11** (1986) 533.
[2] B. E. Conway, L. Bai and M. A. Sattar, *ibid.* **12** (1987) 607.
[3] H. Wendt and U. Plzak, *Electrochim. Acta* **28** (1983) 27.
[4] D. R. Gabe, *Metallurgist* **5** (1973) 72.

[5] B. V. Tilak, P. W. T. Lu, J. E. Colman and S. Srinivasan, in 'Comprehensive Treatise of Electrochemistry', Vol. II (edited by J. O'M. Bockris, B. E. Conway, E. Yeager and R. White), Plenum, New York (1981) p. 1.
[6] B. E. Conway, L. Bai and D. F. Tessier, *J. Electroanal. Chem.* **161** (1984) 39.
[7] S. Srinivasan, H. D. Hurwitz and J. O'M. Bockris, *J. Chem. Phys.* **46** (1967) 3108.
[8] B. V. Tilak, S. Venkatesh and S. K. Rangarajan, *J. Electrochem. Soc.* **136** (1989) 1977.
[9] M. R. Gennero de Chialvo and A. C. Chialvo, *Electrochim. Acta* **35** (1990) 437.
[10] M. A. Devanathan and M. Selvaratnam, *Trans. Faraday Soc.* **56** (1960) 1820.
[11] H. Kita and T. Yamazaki, *J. Res. Inst. Catal. Hokkaido Univ.* **11** (1963) 10.
[12] A. M. Ivanov, L. A. Salnikov, L. P. Timofeeva and L. D. Favorskaya, *Elektrokhimiya* **21** (1985) 1287.
[13] K. Machida, M. Enyo, G. Adachi and J. Shiokawa, *Electrochim. Acta* **29** (1984) 807.
[14] R. S. Schrebler Guzman, J. R. Vilche and A. J. Arvia, *J. Electrochem. Soc.* **125** (1978) 1578.
[15] B. Beden, D. Floner, J. M. Leger and C. Lamy, *Surf. Sci.* **149** (1985) 822.
[16] A. P. Brown, M. Krumpelt, R. O. Loutfy and N. P. Yao, *J. Electrochem. Soc.* **129** (1982) 2481.
[17] S. Maximovitch and R. Durand, *J. Electroanal. Chem.* **149** (1983) 273.
[18] K. Machida and M. Enyo, *J. Res. Inst. Catal. Hokkaido Univ.* **32** (1984) 37.
[19] K. Lohrberg and P. Kohl, *Electrochim. Acta* **29** (1984) 1557.
[20] S. M. Piovano, A. C. Chialvo, W. E. Triaca and A. J. Arvia, *J. Appl. Electrochem.* **17** (1987) 147.